Inorganic Nanoparticles for MRI Contrast Agents

By *Hyon Bin Na, In Chan Song,* and *Taeghwan Hyeon**

Various inorganic nanoparticles have been used as magnetic resonance imaging (MRI) contrast agents due to their unique properties, such as large surface area and efficient contrasting effect. Since the first use of superparamagnetic iron oxide (SPIO) as a liver contrast agent, nanoparticulate MRI contrast agents have attracted a lot of attention. Magnetic iron oxide nanoparticles have been extensively used as MRI contrast agents due to their ability to shorten T2* relaxation times in the liver, spleen, and bone marrow. More recently, uniform ferrite nanoparticles with high crystallinity have been successfully employed as new T2 MRI contrast agents with improved relaxation properties. Iron oxide nanoparticles functionalized with targeting agents have been used for targeted imaging via the site-specific accumulation of nanoparticles at the targets of interest. Recently, extensive research has been conducted to develop nanoparticle-based T1 contrast agents to overcome the drawbacks of iron oxide nanoparticle-based negative T2 contrast agents. In this report, we summarize the recent progress in inorganic nanoparticle-based MRI contrast agents.

1. Introduction

Imaging has been widely used in scientific and technological applications due to its visual and intuitional interface.[1] In particular, biological imaging has been a rapidly growing field, not only in fundamental biology but also in medical science. Although there are many existing imaging tools, new and improved techniques are continually being developed for a wide range of biomedical applications. When a new imaging technique is developed, it ideally exceeds the limitations of its predecessors. However, new imaging tools (or even device upgrades) usually require a large amount of effort and resources before they can be placed in laboratories or hospitals. In economical and practical terms, it is more feasible to develop supplements that can maximize the ability of the current devices or imaging tools. One of the most effective supplements is a chemical compound known as an imaging probe or contrast agent, which is introduced to improve its visibility in the image. Therefore, with the development of imaging tools, many researchers have been trying to design complementary imaging probes or contrast agents to improve the sensitivity and detectability of the tools. With this technological advantage, biological and functional information can be obtained in image form as a result of the interrelation of the contrast agent and the biological system. Without the contrast agent, such information-rich images would be unobtainable. Therefore, imaging probes and contrast agents are an essential research field in biological and medical sciences, to supply a vision for the analysis of biological information and the diagnosis of diseases.

Recently, biomedical imaging has received enormous attention due to its analytic and diagnostic ability at the molecular or cellular level. As a result, a new discipline, known as ''molecular imaging'', which combines molecular biology and in vivo imaging, has emerged.[2] Representative imaging platforms include computed X-ray tomography (CT), optical imaging, magnetic resonance imaging (MRI), positron emission tomography (PET), single-photon-emission computed tomography (SPECT), and ultrasound.[2b] These imaging techniques allow real-time visualization of cellular functions of living organisms and related molecular interactions, and, importantly, they are noninvasive. They can help diagnose diseases, such as cancers and neurodegenerative diseases, and give biological information and functions at preclinical stages.

Most presently available imaging probes and contrast agents are chemical or radioactive agents.[2b,3] However, the tremendous recent advances in nanotechnology have led to the development of new types of probes based on nanoparticles. The properties of such nanoscale materials, especially those of particles smaller than 100 nm, are very different from their bulk counterparts for two main reasons: the increased relative surface area, and the dominant quantum confinement effects. The dramatic increase in the surface area also increases the material's chemical reactivity and ability to connect with additional functional materials. Moreover, quantum-confinement effects, derived from the nanometer particle size, can exert size-dependent electronic, magnetic, and optical properties. Among various forms of probes, inorganic nanometer-sized colloidal particles (nanoparticles) have been extensively used in many imaging systems because of their many useful electronic, optical, and magnetic properties, which are derived from their compositions and nanometer sizes.[4]

[*] Prof. T. Hyeon, Dr. H. B. Na
National Creative Research Initiative Center for Oxide Nanocrystalline Materials
School of Chemical and Biological Engineering
Seoul National University
Seoul 151-744 (Korea)
E-mail: thyeon@snu.ac.kr
Prof. I. C. Song
Department of Radiology
Seoul National University Hospital
Seoul 110-744 (Korea)

DOI: 10.1002/adma.200802366

Semiconductor nanoparticles (also known as quantum dots) have been used as fluorescent probes for cell labeling in optical imaging,[5] and gold nanoparticles have been investigated due to their unique surface plasmon resonance (SPR) in optical imaging and sensing.[6]

MRI is currently one of the most powerful diagnosis tools in medical science.[7] It has been the preferred tool for imaging the brain and the central nervous system, for assessing cardiac function, and for detecting tumors. Since it can give anatomic images of soft tissue with high resolution, it is expected to become a very important tool for molecular and cellular imaging.[2] For instance, it may be useful for the early detection of lesions. Although MRI itself gives detailed images, making a diagnosis based purely on the resulting images may not be accurate, since normal tissues and lesions often show only small differences in relaxation time. MRI contrast agents, which can help to clarify images, allow better interpretation. Most presently available MRI contrast agents are paramagnetic complexes, usually gadolinium (Gd^{3+}) chelates.[3] Amongst them, Gd-DTPA has been the most widely used. Its main clinical applications are focused on detecting the breakage of the blood brain barrier (BBB) and on changes in vascularity, flow dynamics, and perfusion. Superparamagnetic iron oxide (SPIO) is a different class of contrast agents, and it has received great attention since its development as a liver contrasting agent 20 years ago.[8] It was the first nanoparticulate MRI contrast agent, and is still used clinically. Gd-based contrast agents enhance the signal in T1-weighted images.[3] On the other hand, SPIO provides a strong contrast effect in T2-weighted images, due to its different contrasting mechanism.[8] Furthermore, its nanoparticulate properties represented by the nanosized dimension and shape allow different biodistribution and opportunities beyond the conventional imaging of chemical agents. The recent development of molecular and cellular imaging, which enables visualization of the disease-specific biomarkers at the molecular and cellular levels, has led to increased recognition of nanoparticles as MRI contrast agents, where nanoparticulate iron oxide has been the prevailing and only clinically used nanoparticulate agent. However, as a result of the tremendous progress in nanotechnology, many researchers have recently developed new nanoparticulate MRI contrast agents that have further improved contrasting abilities and have extra functions. In the following sections, we review the recent progress in MRI contrast agents based on nanoparticles. These nanoparticle-based MRI contrast agents are composed of three parts: i) the core nanoparticles, which generate the signal enhancement, ii) the water-dispersible shells, which endow compatibility in the biological environment, and iii) the bioactive materials for targeting purpose (Fig. 1). In particular, this report is focused on the core nanoparticles and the biocompatible shells.

Hyon Bin Na received his BS (2001) and PhD (2008) in chemical engineering from Seoul National University, Korea. During his PhD course under the direction of Prof. Taeghwan Hyeon, he first studied the synthesis of inorganic nanoparticles using a chemical process, and then focused on biomedical applications of biocompatible nanoparticles, in particular, bioimaging, such as magnetic resonance imaging. He is currently a postdoctoral researcher working with Prof. Taeghwan Hyeon at Seoul National University.

In Chan Song is a Professor in the department of Radiology at Seoul National University Hospital. He received his BS (1985) and MS (1988) in physics and his PhD (1996) in biophysics in the department of microbiology from the Seoul National University, Korea. His research focuses on the basic and clinical applications of quantitative MRI, perfusion MR imaging, diffusion tensor imaging, and molecular imaging using magnetic resonance imaging.

Taeghwan Hyeon is the Director of the National Creative Research Initiative Center for Oxide Nanocrystalline Materials and a Professor of the School of Chemical and Biological Engineering at Seoul National University. He received his BS (1987) and MS (1989) in chemistry from the Seoul National University, Korea, and his PhD in chemistry from the University of Illinois at Urbana-Champaign (1996). His research focuses on the synthesis and applications of uniform-sized nanocrystals and nanoporous materials.

2. Basic Principles of MRI Contrast Agents

'Contrast' refers to the signal differences between adjacent regions, which could be 'tissue and tissue', 'tissue and vessel', and 'tissue and bone'. Contrast agents for X-ray and CT show contrasting effects according to the electron-density difference, and they produce direct contrast effects on their positions. However, the contrast mechanism is more complicated for MRI, where the contrast enhancement occurs as a result of the interaction between the contrast agents and neighboring water protons, which can be affected by many intrinsic and extrinsic factors such as proton density and MRI pulse sequences. The basic principle of MRI is based on nuclear magnetic resonance (NMR) together with the relaxation of proton spins in a magnetic field.[7] When the nuclei of protons are exposed to a strong magnetic field, their spins align either parallel or antiparallel to the magnetic field. During their alignment, the spins precess under a specified frequency, known as the Larmor frequency (ω_0, see Fig. 2a). When a 'resonance' frequency in the radio-frequency (RF) range is introduced to the nuclei, the

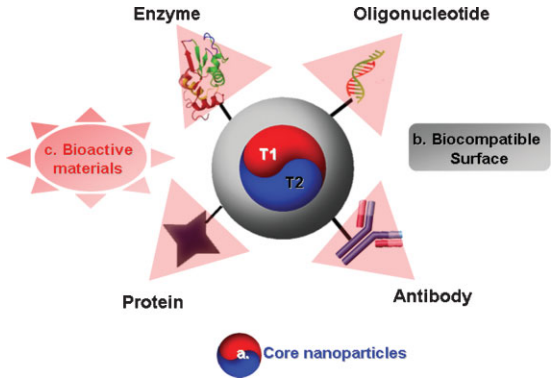

Figure 1. The structure of MRI contrast agent based on nanoparticles.

protons absorb energy and are excited to the antiparallel state. After the disappearance of the RF pulse, the excited nuclei relax to their initial, lower-energy state (Fig. 2b). There are two different relaxation pathways. The first, called longitudinal or T1 relaxation, involves the decreased net magnetization (M_z) recovering to the initial state (Fig. 2c). The second, called transverse or T2 relaxation, involves the induced magnetization on the perpendicular plane (M_{xy}) disappearing by the dephasing of the spins (Fig. 2d). Based on their relaxation processes, the contrast agents are classified as T1 and T2 contrast agents. Commercially available T1 contrast agents are usually paramagnetic complexes, while T2 contrast agents are based on iron oxide nanoparticles, which are the most representative nanoparticulate agents.

3. T2 Nanoparticulate MRI Contrast Agents

When a RF pulse is applied to spins, transverse magnetization on the *xy*-plane (M_{xy}) perpendicular to the direction of the static magnetic field is generated (Fig. 2b). Net magnetization **M** as a vector has the components of M_z and M_{xy}, which produce the interrelated process of spins. The change in M_z is due to energy transfer, whereas that in M_{xy} is due to the process of spin dephasing, that is, the randomization of the magnetization of excited spins with the same phase coherence immediately after the application of an RF pulse. Their phase coherence in *xy*-plane disappears due to the difference of magnetic field experienced by the protons. The magnetic-field difference is produced by the system performance in shimming and the magnetic properties of imaging objects. Although the inhomogeneity of the static magnetic field by the system imperfection can be reduced by a variety of tools, including shimming coils and shimming algorithms and the usage of the spin echo sequence to reverse this effect, it affects the decay of transverse magnetization. As another source of field inhomogeneity, the magnetic properties of imaging objects can cause phase incoherence. The spin–spin interaction between the hydrogen nuclei or electrons causes a loss of transverse coherence, which produces the true and characteristic T2 relaxation of tissues. For example, the proton interaction of macromolecules in tissue can induce a local magnetic field, as well as a change in the actual magnetic field in their vicinity. Furthermore, local magnetic field gradients can be induced from the differences in the magnetic susceptibility between the adjacent and different tissues or by contrast agents. Therefore, transverse relaxation is affected by inhomogeneous magnetic fields produced from tissue-inherent factors or external sources, and the total relaxation time, T_2* is described by:

$$\frac{1}{T_2{}^*} = \frac{1}{T_2} + \gamma B_S \tag{1}$$

where γB_S represents the relaxation by the field inhomogenites and is called susceptibility effect.

The magnetization of paramagnetic materials, such as gadolinium complexes, is directly dependent on the number of ions, and they have no magnetization in the absence of an external magnetic field. However, ferromagnetic iron oxide has a very large magnetic susceptibility, which can persist even upon removal of the external magnetic field. Nanosized iron oxide particles are superparamagnetic, losing their magnetization in the absence of an external magnetic field. However, when an external magnetic field is applied, they exhibit strong magnetization, which can cause microscopic field inhomogeneity and activate the dephasing of protons. Therefore, iron oxide nanoparticles shorten T2 and T2* relaxation times of the neighboring regions, and produce a decreased signal intensity in T2- and T2*-weighted MR images.

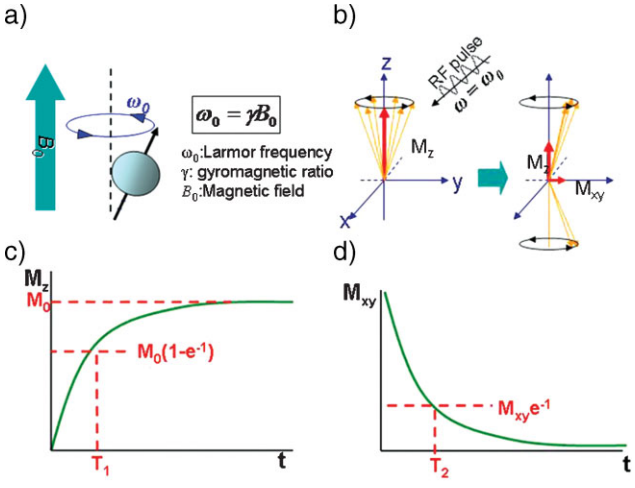

Figure 2. Principle of magnetic resonance imaging. a) Spins align parallel or antiparallel to the magnetic field and precess under Larmor frequency (ω_0). b) After induction of RF pulse, magnetization of spins changes. Excited spins take relaxation process of c) T1 relaxation and d) T2 relaxation.

3.1. Dextran-Coated Iron Oxide Nanoparticles

Since their first use as MRI contrast agents 20 years ago, iron oxide nanoparticles (usually magnetite (Fe_3O_4) or maghemite (γ-Fe_2O_3)) have become extremely popular due to their ability to dramatically shorten T2* relaxation times in the liver, spleen, and bone marrow by selective uptake and accumulation in the cells of the reticuloendotherial system (RES).[8] With their high

Table 1. Properties of T2 contrast agents.

Name	Core Material	Surface	Diameter of Core [nm]	Hydrodynamic Diameter [nm]	Magnetization [emu g^{-1}][a]	r_2 [mM^{-1} s^{-1}]	B_0 [T]	Reference
Ferumoxides (Feridex)	Fe_3O_4, γ-Fe_2O_3	Dextran	4.96	160	45	120	1.5	10a
Ferucarbotran (Resovist)	Fe_3O_4	Carboxydextran	4	60		186	1.5	10b
Ferumoxtran (Combidex)	Fe_3O_4	Dextran	5.85	35	61	65	1.5	10b
CLIO-Tat	Fe_3O_4	Dextran	5	30	60	62	1.5	15a
WSIO (MEIO)	Fe_3O_4	DMSA[b]	4		25	78	1.5	20b,21b
			6		43	106		20b,21b
			9		80	130		20b,21b
			12		101	218		20b,21b
FeNP	α-Fe	PEG	10		70	129	1.5	23
MnMEIO	$MnFe_2O_4$	DMSA[b]	6		68	208	1.5	21b,24
			9		98	265		21b,24
			12		110	358		21b,24
CoMEIO	$CoFe_2O_4$	DMSA[b]	12		99	172	1.5	21b,24
NiMEIO	$NiFe_2O_4$	DMSA[b]	12		85	152	1.5	21b,24
Au-Fe_3O_4	Fe_3O_4	PEG	20			114	3.0	41a
Au-FePt	FePt (fcc)	PEG	6			59	3.0	41b

[a] Magnetic properties were measured at 1.5 T external field. [b] 2,3-Dimercaptosuccinic acid.

magnetization, their selective signal loss allowed for a new class of MRI contrast agents in the world of dominant T1 contrast agents based on ionic complexes. Since the biological distribution of the nanoparticles is directly dependent on their size, they have been classified by size as follows: i) micrometer-sized paramagnetic iron oxide (MPIO; several micrometers), ii) superparamagnetic iron oxide (SPIO; hundreds of nanometers), and ultimately, iii) ultrasmall superparamagnetic iron oxide (USPIO; less than 50 nm).[9] The most representative and traditional method of preparing SPIOs and USPIOs is by the reduction and coprecipitation reaction of a mixture of ferrous and ferric salts in aqueous media in the presence of stabilizers such as hydrophilic polymers.[10] This process was adapted for several commercial MRI contrast agents based on iron oxide nanoparticles, such as Feridex, Resovist, and Combidex, which are SPIO or USPIO agents. These particles consist of multiple iron oxide cores within a dextran stabilization shell. Table 1 summarizes the physical and chemical properties of dextran-stabilized iron oxide nanoparticles. The usual clinical targets of SPIO have been liver diseases,[8] because SPIO is selectively taken up by the Kupffer cells in the liver, spleen, and bone marrow. If the normal liver architecture is destructed by a hepatic disease, such as a primary liver tumor or liver metastasis, the region will have a lack of Kupffer cells. Due to the negligible uptake by the abnormal liver, the SPIO presents a strong contrast between normal and abnormal tissues, thereby enabling clear detection of the abnormal tissue. However, SPIO's rapid uptake by the liver leads to its fast excretion from blood plasma, which induces a limitation in SPIO's ability to depict the molecular and biological functions in MRI.

The size of particles is the main factor that controls their characteristics, such as blood half-life and biodistribution. Small nanoparticles have a longer plasma-circulation time, due to their slow excretion by the liver. Therefore, iron oxide nanoparticles for molecular imaging are usually in the USPIO class (<50 nm). A typical clinical application of USPIOs is lymph-node imaging.[11] The detection of lymph nodes is critical for accurate tumor staging and the subsequent therapeutic planning. Since USPIOs are very small, they can be extravazated from the blood vessels into interstitial spaces, and they are transported to lymph nodes through lymphatic vessels (Fig. 3a). As nodes that have malignant cells cannot undergo phagocytosis by nodal macrophages, nanoparticles are uptaken only by the normal nodes. Their accumulation within normal nodes produces significant susceptibility effects, and the specific uptake allows a more sensitive detection between normal and malignant cells. Therefore, they are expected to improve the diagnosis of metastatic tumors, and are currently under investigation for human applications. For instance, Weissleder and coworkers reported the successful detection of lymph-node metastases in patients with prostate cancer using USPIO (Fig. 3b).[11] USPIOs have been tested as blood-pool agents because they are readily distributed in the intravascular extracellular space. For example, many clinicians have tried to use USPIOs for angiography, functional MRI (fMRI), and passive targeted imaging of tumors.

However, the aforementioned applications are based mainly on the biological behavior of iron oxide nanoparticles. In view of molecular imaging, recent interest has been focused on active imaging with maximization of nanoparticulate features. As mentioned in the introduction, nanoparticles have advantages over paramagnetic complex agents. Nanosized particles can be easily uptaken by both macrophage cells and nonphagocytic cells. Moreover, targeted imaging is possible because nanoparticles have a large surface area that can be conjugated with biological and targeting probes, such as antibodies, oligonucleotides, aptamers, and other imaging probes. Iron oxide nanoparticles have shown outstanding results in the field of target-specific in vivo or in vitro imaging, in particular in monitoring the migration and tracking of cells, and in disease-targeted imaging.

Cell therapy is a personalized treatment that has been used for more than 50 years. In particular, recent research on stem cells gives hope to those suffering from incurable diseases. For successful cell therapy and the monitoring of cell tracking and differentiation in vivo, it is critical to develop methods for the noninvasive assessment of the fate and distribution of cells.

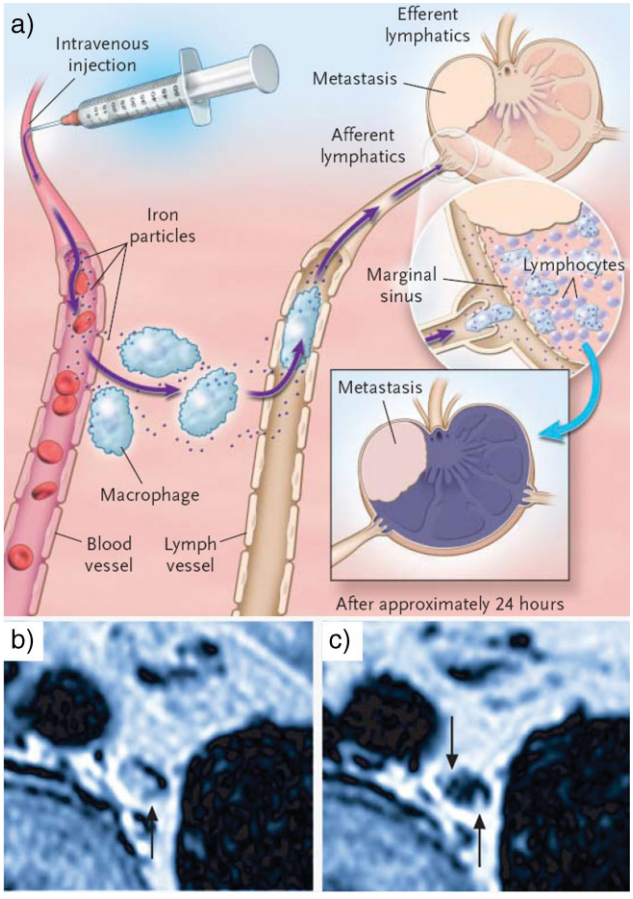

Figure 3. a) Mechanism of action of ultrasmall superparamagnetic iron oxide nanoparticles. b,c) MR images of a metastatic lymph node b) before and c) after USPIO. Reproduced with permission from [11]. Copyright 2003 Massachusetts Medical Society.

Because the magnetic nanoparticles' large susceptibility provides highly sensitive tracking with very low detection limits, and their use enables the labeling of target cells with high efficiency, in vivo MR imaging of ex vivo labeled cells with SPIO and USPIO has been used. MR anatomic imaging using SPIO and USPIO has been used for phagocytic cells, such as neutrophils, macrophages, and monocytes, and for nonphagocytic cells, such as lymphocytes, glioma cells, and stem cells.[9] In the initial studies, those cells were labeled by simple incubation with a high concentration of native nanoparticles. Because simple incubation has the limitations of long incubation time and low labeling efficiency in the case of the nonphagocytic cells, various chemical, mechanical, and biological approaches were developed to deliver the nanoparticles efficiently into the cells.[12–15] First, the use of transfection agents and electroporation were adapted from the methods used to introduce DNA or plasmids.[13] Bulte et al. reported the efficient labeling of stem cells with magnetic iron oxide through electromagnetoporation, which combines the electromechanical permeability changes of the cellular membrane and the accelerated movements of iron oxide in a magnetic field.[14] Another approach is the modification of nanoparticles with the attachment of biomaterials that facilitate particle binding to the anionic cellular membrane, followed by internalization. Viruses, peptides, proteins, and antibodies have been conjugated or coated with USPIO and SPIO.[15] In particular, dextran-stabilized monocrystalline iron oxide nanoparticles (MION) were popularly conjugated to biomaterials because MION can be readily functionalized with amine groups by epichlohydrin treatment. Josephson et al. reported that crosslinked iron oxide nanoparticles conjugated with HIV-Tat proteins (CLIO-Tat) showed efficient nonphagocytic cell labeling through activated macropinocytosis.[15a] The facile process of functionalizing dextran-stabilized iron oxide nanoparticles with amine groups (crosslinked iron oxide, CLIO) established a platform for active molecular imaging. Many kinds of biomolecules, including antibodies, proteins, peptides, polysaccharides, and aptamers, were covalently bound on the surface of the iron oxide nanoparticles for their site-specific accumulation at the targets of interest. Kang et al. reported antibody-conjugated CLIO and in vitro-targeted MR imaging of E-Selectin in endothelial cells.[16] Furthermore, amine groups can be conjugated with small molecules, such as optical dyes for multimodal imaging and synthetic ligands to develop targeted-imaging and therapeutic materials with rapid screening and imaging.[17,18] Weissleder and coworkers developed biocompatible magnetic relaxation switches (MRS) to detect molecular interactions, such as DNA–DNA, protein–protein, protein–small molecule, and enzyme reactions,[18] based on the observation that self-assembled magnetic nanoparticles exhibited enhanced spin–spin relaxation times (T2) compared to the individual magnetic nanoparticle dispersions.

3.2. New MRI Contrast Agents Based on Magnetic Nanoparticles

As described in the previous section, dextran-based iron oxide nanoparticles (SPIO, USPIO) have been applied to conventional clinical imaging and molecular imaging for the last 20 years. However, they have some limitations originated from their synthetic processes. They were generally synthesized by a coprecipitation reaction in water at a relatively low temperature, resulting in the formation of polydisperse and poorly crystalline nanoparticles with inferior magnetic properties. For molecular and cellular imaging, high resolution and sensitivity are required to fulfill the quantization and interpretation issues. In general, nanoparticles have to meet the following requirements for their applications to biomedical imaging agents. First, nanoparticles have to possess suitable properties for the contrasting mechanism. Second, they should be compatible with biological systems. Finally, they should have reactive moieties on the surface for the conjugation with biological active materials. In general, the contrasting ability originates from the core materials, whereas the biocompatibility and conjugation capability are related to the surface properties. Recently numerous studies have been conducted to develop new MRI contrast agents based on magnetic nanoparticles, with core materials with improved magnetic properties and suitable surface characteristics. In the following, we will discuss these two issues separately: core materials and surface functionalization.

3.2.1. Magnetic Nanoparticles with Improved Magnetic Properties

Acceleration of spin–spin relaxation (T2 shortening) by magnetic nanoparticles results from the dephasing of the magnetic moments due to the magnetic-field gradients created by the small magnetized particles. In this process, the major relaxation mechanism is the dipolar outer-sphere interaction between the water proton spins and the magnetic moment of the nanoparticles. Therefore, as shown in the model suggested by Koenig and Keller, spin–spin relaxation is dependent on the magnetic moment of the nanoparticles (μ):[19]

$$R_2 = \frac{1}{T_2} = \frac{a}{d_{NP}D}\gamma^2\mu^2 C_{NP} J(\omega, \tau_D) \quad (2)$$

where a is a constant, d_{NP} the diameter of the nanoparticle, D the diffusion coefficient, μ the magnetic moment of the nanoparticles, γ the gyromagnetic ratio of the water proton, C_{NP} the concentration of the nanoparticles, and $J(\omega,\tau_D)$ the spectral density function.

In other words, to be efficient T2 contrast agents, nanoparticles should possess a large magnetization. Although magnetism is an intrinsic property of bulk materials, the magnetic properties of nanoparticles are strongly dependent on their size, shape, and surface property.[20] A dramatic increase in surface area induces preponderant surface-canting effects, and consequently increases the magnetization, as described by the following equation:[21]

$$m_S = M_S[(r-d)/r]^3 \quad (3)$$

where m_S is the saturation magnetization of the nanoparticle, M_S the saturation magnetization of the bulk material, r the size of the nanoparticle, and d the thickness of the disordered surface layer.

To produce efficient T2 contrast agents, we have to control the magnetic properties of the nanoparticles through the designed control of i) the intrinsic material properties, such as material composition and crystal structure, and ii) extrinsic factors, such as size and shape.[21c]

Most T2 contrast agents are based on iron oxide nanoparticles, and are composed of aggregated nanoparticles with multiple iron oxide (4–5 nm) cores and dextran coatings. USPIOs with a single core (MION, CLIO) have low relaxivities due to their small core size. Monodisperse and highly crystalline iron oxide nanoparticles have been synthesized by various synthetic methods in the last decade.[4j,22] The most representative method is thermal decomposition of metal precursors in organic surfactant solutions at a high temperature of $>300\,^{\circ}C$ (Fig. 4a). The resulting hydrophobic nanoparticles had uniform sizes ($\sigma < 10\%$), which were finely controlled by simple alterations of synthetic parameters (4–25 nm). In particular, Hyeon et al. reported the large-scale production of various metal oxide nanoparticles including iron oxide from the thermal decomposition of metal–surfactant complexes that were generated from the reaction of inexpensive and nontoxic metal salts with surfactants.[22c] Recently, some of these uniform-sized iron oxide nanoparticles have been used for MRI contrast agents.

Cheon and coworkers systematically studied the relationships between size, magnetism, and relaxivity of uniform-sized iron oxide nanoparticles (Table 1).[20b] Large iron oxide nanoparticles have a large magnetization and high r_2 relaxivity, which renders it possible to increase the sensitivity in T2/T2*-weighted images and to ease the toxicity concern by decreasing the agent dose. Because magnetism is an intrinsic property of materials, magnetic nanoparticles with high magnetism have recently been synthesized to develop new MRI contrast agents with improved relaxation properties and biocompatibility. Hadjipanayis and coworkers reported that iron nanoparticles had larger T2 relaxivity than iron oxide nanoparticles of comparable size.[23] They also demonstrated that the large magnetization of the iron nanoparticles could induce effective local hyperthermia.

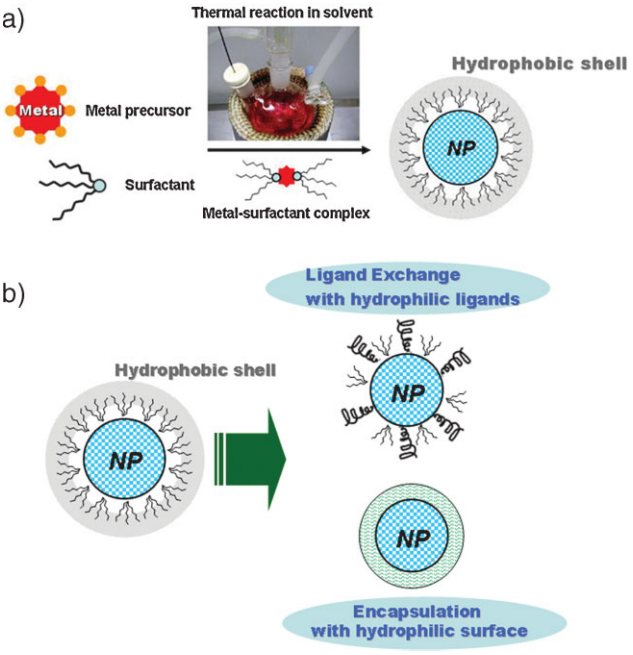

Figure 4. Synthesis of biocompatible nanoparticles. a) Reaction scheme for monodisperse nanoparticles by thermal reaction under surfactant. b) Surface modification of hydrophobic nanoparticles.

Alloy materials can be candidates for more-efficient T2 contrast agents. Various bimetallic ferrite nanoparticles, including $CoFe_2O_4$, $MnFe_2O_4$, and $NiFe_2O_4$, have been tested for T2 contrast agents. The $MnFe_2O_4$ nanoparticles (MnMEIO) have been found to have a very high magnetization (Table 1) and large relaxivity (Fig. 6).[24]

3.2.2. Biocompatible Surface and New Ligands

For many biomedical applications, in particular for in vivo imaging, nanoparticles should possess good colloidal stability and low toxicity in a biological environment. Although high-quality magnetic nanoparticles with uniform size and high crystallinity were synthesized from thermal decomposition of metal precursors in organic media, they are hydrophobic, and consequently are not sufficiently stable in aqueous media for biomedical applications.[4] Therefore, modifying the surface of these nanoparticles is essential to endow them with hydrophilic properties, so that they can be extensively used for various biomedical applications.[25] Furthermore, surface modification is important for the nanoparticles to impart additional functions,

because bioactive materials are conjugated through the reactive groups on the surface. Recently, various surface-modification methods were developed, and two representative strategies are ligand exchange with water-dispersible ligands and encapsulation with biocompatible shells (Fig. 4b).

Nanoparticles prepared in organic solvents are stabilized by surfactants that have their hydrophilic head groups bound to the surface of the nanoparticles and the hydrophobic hydrocarbon tails facing the solvent (Fig. 4a). Since the atoms on the surface of the nanoparticles have an affinity for the functional groups, surface functionalization with proper hydrophilic ligands allows the phase transfer of nanoparticles from organic media to aqueous media. Various kinds of nanoparticle can undergo substitution reactions with excess bifunctional ligands, which consist of a strong binding moiety to the surface of the nanoparticles and relatively low binding hydrophilic group. These ligand-exchange methods have several advantages, including simple procedure, thin passivating layer, and small overall size. Because metal oxide nanoparticles have relatively unreactive surfaces compared to other kinds of nanoparticles, such as chalcogenide-based quantum dots, there is a very limited number of functional groups available. For example, metal oxide nanoparticles do not bind strongly to alkanethiols, which serve as excellent ligands for nanoparticles of chalcogenides and metals. Consequently, there has been intensive recent research on the development of new ligand systems that can bind strongly to metal oxide nanoparticles, in particular, iron oxide nanoparticles. Dopamine was used as a ligand to immobilize functional molecules on iron oxide nanoparticles,[26a,b] whereas Peng and coworkers took advantage of the interaction between hydroxamic acid and iron oxide.[26c] Cheon and coworkers were able to form water-dispersible iron oxide nanoparticles using a small organic molecule, 2,3-dimercaptosuccinic acid (DMSA), which has a bidentate carboxyl group.[20b] The resulting iron oxide nanoparticles were dispersible in water and were successfully used for in vivo MRI. To improve the biocompatibility of the nanoparticles, the backbones of the ligands were designed to contain biocompatible polymers, such as poly(ethylene glycol) (PEG). PEG-derivatized phosphine oxide ligands (PO-PEGs) consisted of a biocompatible PEG tail group, and a surface-coordinating phosphine oxide head group could stabilize several kinds of oxide nanoparticles in aqueous media.[26d] They were prepared by simple reaction between $POCl_3$ and PEGs. Polymeric or dendrimeric ligands have also been used for the stabilization of iron oxide nanoparticles in aqueous media derived from their multiple functional groups and bulky structures.[26e] These ligands interact through a number of bonds on the nanoparticles by ligand exchange.

The second strategy for surface modification is the formation of biocompatible shells around the nanoparticles. Although there are a variety of biocompatible-shell-formation methods, they can be broadly classified according to the shell materials and the encapsulation processes. Typical shell materials are silica and polymers. Crosslinked amorphous silica shells can stabilize oxide nanoparticles. Although the toxicity of nanosized silica is still in debate, there have been promising in vitro and in vivo reports on silica-encapsulated nanoparticles.[4a,27] Ying and coworkers reported on silica-coated nanoparticles produced by base-catalyzed silica formation in a reverse microemulsion.[27] Although the silica layer is relatively thick (10–30 nm), the encapsulation process is simple and various kinds of nanoparticle can be encapsulated. It also allows the encapsulation of multiple nanoparticles within one shell. However, the silica shells have charges, and are sensitive to the pH of the surrounding medium, which can cause precipitation and gel formation. More recently, additional biocompatible polymers (e.g., PEG) have been impregnated onto the surface of the silica shell to improve colloidal stability.[28]

Various natural and synthetic polymers have been extensively used in biomedical areas. The immobilization of magnetic nanoparticles in clinically used polymers can reduce the safety and toxicology concerns. Furthermore, these polymer–nanoparticle hybrids can be utilized for multifunctional biomedical applications with simultaneous drug-delivery and imaging capabilities.[29] Polyesters, such as poly(D,L-lactide-*co*-glycolide) (PLGA), poly(D,L-lactide) (PLA), and poly(glycolide) (PGA), have been most popularly used for these applications.[30] Kim et al. fabricated multifunctional PLGA nanoparticles with particle sizes of 100–200 nm by simultaneously immobilizing magnetite nanoparticles, quantum dots, and an anticancer drug (doxorubicin) in a PLGA matrix via a conventional oil-in-water emulsion–evaporation process.[29a] Using the multifunctional polymer nanoparticles, they demonstrated simultaneous cancer-targeted MR imaging, optical imaging, and drug delivery. In addition, the loaded magnetite nanoparticles facilitated the magnetic guiding of the polymer particles, thereby increasing the synergetic targeting efficiency. Jiang and coworkers fabricated hollow Fe_3O_4–polymer hybrid nanospheres by addition of Fe_3O_4 nanoparticles to an aqueous solution of polymer–monomer pairs composed of cationic chitosan and anionic acrylic acid monomer, followed by polymerization of acrylic acid and selective crosslinking of chitosan at the end of polymerization.[29b,c] The phantom test of magnetic resonance imaging showed that the synthesized hybrid hollow nanospheres had a significant magnetic-resonance signal enhancement in T2-weighted images.[29c]

PEG, a representative biocompatible polymer, has received great attention due to its nonfouling property, which supports a resistance to protein adsorption and an ability to bypass the RES and natural barriers, such as the nasal mucosa.[31] PEGs have been extensively used as stabilizing materials for many nanoparticles used in biomedical applications, in particular in long circulating in vivo imaging systems. Because PEG itself is very inert, surface-anchorable materials, such as copolymers, phospholipids, and silica, are combined with PEGs to encapsulate the nanoparticles. Dubertret et al. reported that PEG–phospholipid block-copolymers could form a stable micelle structure on quantum dots via the hydrophobic interaction between hydrophobic tail groups of the surfactants and phospholipid parts.[5d] The outer surface of the nanoparticles is comprised of a dense PEG layer, which is stable in biological media. This process is highly reliable, and can generally be applicable to many other kinds of nanoparticle. Using a very similar strategy, various water-dispersible metal oxide nanoparticles, including iron oxide nanoparticles, were generated.[32] Because these PEG–phospholipid block copolymers are very expensive, they cannot be applied for large-scale preparation. Amphiphilic di- and triblock copolymers have also been used as

stabilizing shell materials for water-dispersible nanoparticles. Their hydrophobic blocks can strongly interact with the hydrophobic surface of the nanoparticles, whereas the outer hydrophilic blocks can render the nanoparticles dispersible in water.[33] These block copolymers are relatively inexpensive, and can be derivatized with other functional groups for additional functionalization. One disadvantage of using these block copolymers is that their large shell thickness is derived from the high molecular weight, which limits their many potential applications. Oligomeric and dendritic molecules were used as shell materials for water-dispersible nanoparticles because they form thinner shells while preserving their stability in aqueous media. For example, Yang and coworkers demonstrated that the cyclic oligosaccharides that have hydrophobic cavities and hydrophilic rims, can transfer the nanoparticles from an organic to an aqueous phase.[34]

Weller and coworkers showed that the relaxivities of magnetic nanoparticles were dependent not only on the size of the core nanoparticles but also on the types of shells.[35] $MnFe_2O_4$ nanoparticles synthesized in ether were transferred to water using three different approaches, namely ligand exchange to form a water-soluble polymer shell, embedding into an amphiphilic polymer shell, and encapsulating in large micelles formed by lipids. In the first two polymer-based systems, nanoparticles were individually dispersed to form homogenous dispersions with a hydrodynamic radius of 30–40 nm, whereas aggregated nanoparticles were randomly distributed inside the micelles with a hydrodynamic radius of 250 nm. Interestingly, the relaxivity, r_2*, is much higher for the micellar system than for the polymer-stabilized particles using same-sized nanoparticles (Fig. 5).

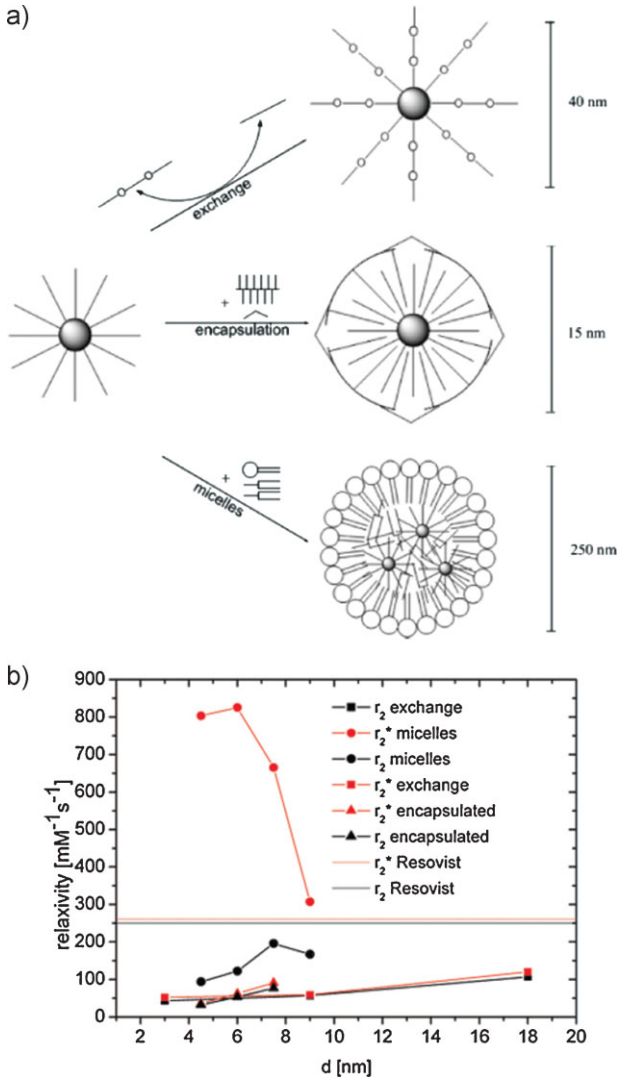

Figure 5. a) Three kinds of methods to prepare water-dispersed manganese ferrite nanoparticles. b) The r_2 relaxities of water-dispersed manganese ferrite nanoparticles with three kinds of shell systems. Reproduced with permission from [35]. Copyright 2007 American Chemical Society.

3.2.3. Multifunctional T2 MRI Agents

Water-dispersed iron oxide nanoparticles have been extensively applied to the diagnosis of cancers. They can be accumulated spontaneously in tumor sites via the enhanced permeability and retention (EPR) effect, which is the enhanced accumulation of macromolecular species, including nanoparticles, in tumor tissues that have abnormal blood vessels.[36] Consequently, iron oxide nanoparticles were successfully used to image tumors without any targeting probes, which are called as passive targeting.[37] For more efficient targeted imaging, the surfaces of the iron oxide nanoparticles need to be conjugated with active targeting probes, such as antibodies and proteins. Cheon and coworkers prepared Herceptin-conjugated iron oxide nanoparticles, and they delivered selectively and imaged tumor cells by the interactions with the human epidermal-growth factor receptor (Her2/neu), which is usually overexpressed in breast cancers.[20b] As another demonstration, Gao and coworkers conjugated a cancer-targeting antibody, anti-carcinoembryonic antigen (CEA) monoclonal antibody rch 24, onto uniform PEG-coated iron oxide nanoparticles, and successfully performed targeted MRI of human colon carcinoma tumors.[38] Zhang and coworkers demonstrated that PEG-coated iron oxide nanoparticles conjugated with targeting peptide (chlorotoxin) were preferentially accumulated within gliomas and exhibited highly contrast-enhanced MR images.[39]

Magnetic nanoparticles with high magnetization showed more sensitive in vivo T2 MR cancer targeted imaging.[24] Herceptin-conjugated manganese ferrite (MnMEIO) nanoparticles showed highly sensitive targeted in vivo mice imaging, enough to detect very small tumors on mice (Fig. 6). This result demonstrated that advanced MRI contrast agents consisting of high-magnetic-moment nanoparticles and appropriate targeting agents could enable the ultrasensitive detection of various types of cancer in T2/T2*-weighted MRI.

Recently, new multifunctional nanomedical platforms were fabricated by combining various nanostructured materials with different functions, rendering it possible to accomplish multimodal imaging and simultaneous diagnosis and therapy.[40] Dumbbell-like nanoparticles composed of magnetic and gold nanoparticles were used for dual MR and optical imaging.[41] The Sun group reported the bimodal imaging properties of Fe_3O_4-Au dumbbell nanoparticles that were prepared by the growth of Fe_3O_4 on as-prepared Au nanoparticles in the presence of oleic

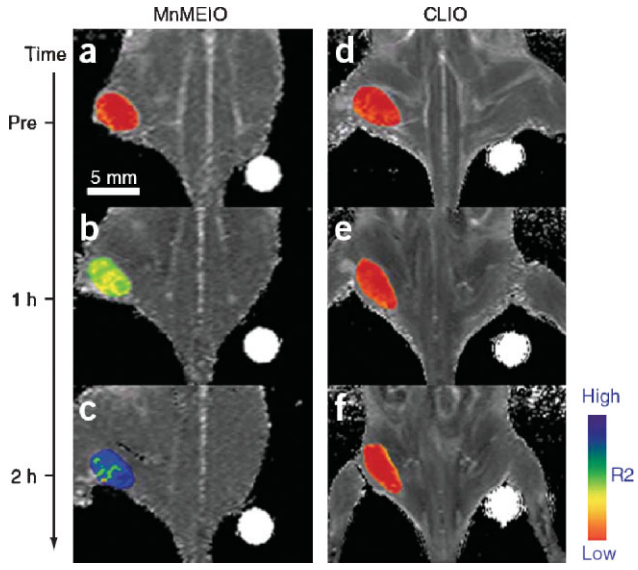

Figure 6. In vivo MR detection of cancer after administration of magnetic nanoparticles-Herceptin conjugates. Manganese ferrite nanoparticles (MnMEIO) a–c) shows higher signal enhancement than d–f) crosslinked iron oxide (CLIO). Reproduced with permission from [24]. Copyright 2007 Nature Publishing Group.

acid and oleylamine (Fig. 7).[41a] The Fe_3O_4 and Au components had different surface properties, and were modified by dopamine and thiol groups, respectively. The epidermal growth factor receptor antibody (EGFRA) was conjugated on the surface of Fe_3O_4, and the resulting heterostructured nanoparticles were successfully applied to the cancer-targeted MR imaging. Furthermore, the unique surface plasmon property of the Au component enabled reflection imaging. The Cheon group demonstrated dual modal imaging using heterodimeric FePt-Au nanoparticles that were synthesized by the catalytic growth of Au on the surface on the FePt nanoparticles.[41b] Antibody-conjugated FePt-Au nanoparticles were used as both T2 MRI contrast agents and biosensors, and neutravidin-conjugated nanoparticles acted as detecting probes on the biotin-patterned biochip.

Piao et al. fabricated biocompatible hollow magnetite nanocapsules via a so-called wrap–bake–peel process, which involves silica coating of akagenite (β-FeOOH) nanorods, heat treatment, and finally the removal of the silica layer. Large hollow pores could be loaded with chemical drugs that were released in cancer cells, and the magnetite shells were used for T2 MRI contrast agent (Fig. 8).[42]

3.3. T1 Nanoparticulate MRI Contrast Agents

Over the last 20 years, most nanoparticulate contrast agents have been T2 contrast agents

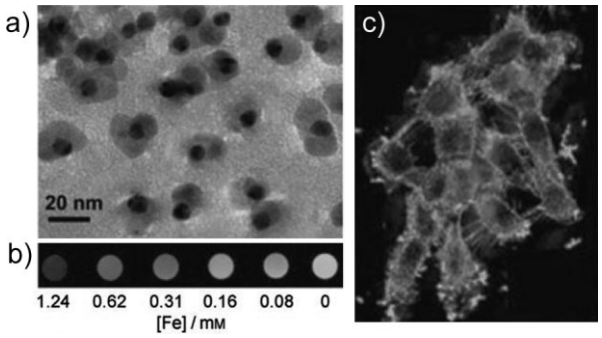

Figure 7. a) TEM image of Au–Fe_3O_4 nanoparticles. b) T2-weighted MR images of A431 cells labeled with Au–Fe_3O_4 nanoparticles. c) Reflection images of A431 cells labeled with Au–Fe_3O_4 nanoparticles. Reproduced with permission from [41a].

using iron oxide nanoparticles. However these magnetic nanoparticle-based agents have several disadvantageous features that limit their extensive clinical applications. First, they are negative imaging agents, which give a signal-decreasing effect. The resulting dark signal could be confused with other pathogenic conditions, and renders images of lower contrast than T1 contrasted images. Moreover, the high susceptibility of the T2 contrast agents induces distortion of the magnetic field on neighboring normal tissues. This distortion of the background is called susceptibility artifact or 'blooming effect', and generates obscure images and demolishes the background around the lesions.[9] Because of the these, most extensively and clinically used MRI contrast agents are based on gadolinium complex-based T1 agents. T1 relaxation is the process of equilibration of

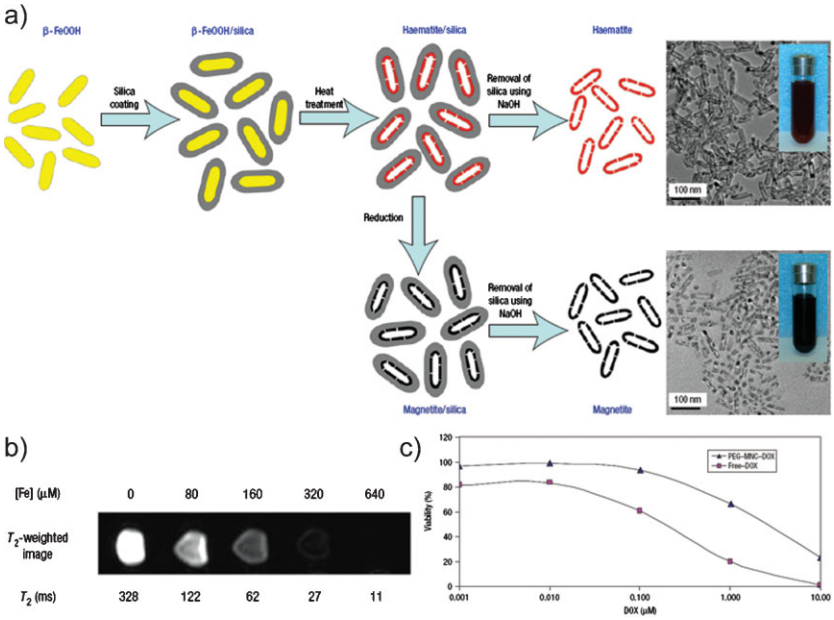

Figure 8. a) Schematic illustration of the procedure for the synthesis of uniform and water-dispersible iron oxide nanocapsules and their TEM images. b) T2-weighted MR images of the magnetite nanocapsules. c) In vitro cytotoxicity of free DOX and DOX loading nanocapsules against SKBR-3 cells. Reproduced with permission from [42]. Copyright 2008 Nature Publishing Group.

	Ion	Configuration 3d	Configuration 4f	Magnetic moment
Transition metal ion	$^{24}Cr^{3+}$	↑↑↑— —		3.88
	$^{25}Mn^{2+}$	↑↑↑↑↑		5.92
	$^{26}Fe^{3+}$	↑↑↑↑↑		5.92
	$^{29}Cu^{2+}$	↑↓↑↓↑↓↑↓↑		1.73
lanthanide metal ion	$^{63}Eu^{3+}$		↑↓↑↑↑↑↑	3.4
	$^{64}Gd^{3+}$		↑↑↑↑↑↑↑	7.94
	$^{66}Dy^{3+}$		↑↓↑↑↑↑↑	10.65

Figure 9. Electron configuration and magnetic moment of metal ions.

the net magnetization (M_z) after the introduction of an RF pulse. This change of M_z is a consequence of energy transfer between the proton spin system and the nearby matrix of molecules. All biological systems are composed of various molecules and organisms, and they have different relaxation behaviors and different T1 relaxation times. The presence of paramagnetic ions near the tissue enhances its relaxation and shortens the T1 relaxation time. In particular, transition and lanthanide metal ions with a large number of unpaired electrons, such as Gd^{3+}, Mn^{2+}, and Fe^{3+}, show very effective relaxation (Fig. 9). T1 contrast agents enhance T1 relaxation, a signal-increasing imaging effect. Compared to T2 contrast agents, the major advantage of T1 contrast agents is positive imaging by signal enhancing, which can maximize the forte of MRI, that is, anatomic imaging with high spatial resolution. Furthermore, their bright signal can be distinguished clearly from other pathogenic or biological conditions. As T1 contrasting agents are basically paramagnetic, they do not disrupt the magnetic homogeneity over large dimensions, which can disturb other anatomic backgrounds.

Since Gd^{3+} has seven unpaired electrons with a large magnetic moment, most T1 contrast agents are Gd^{3+}-based agents. However, due to the toxicity of heavy metal ions, the conventional contrast agents are in the form of ionic complexes with chelating ligands, which are thermodynamically and kinetically stable and less toxic. There is, however, no biochemistry based on gadolinium(III) ion in natural humans. In spite of their fewer unpaired electrons and lower magnetic moments, manganese(II), iron(III), and copper(II) ions could be alternative candidates. Manganese(II) ions, in particular, play various important roles in many biological processes, such as cofactors of enzymes and a release controller of neurotransmitters. Although there are some manganese(II) complex contrast agents, Mn^{2+} itself, in the form of $MnCl_2$ solution, has been most frequently used, and has shown very prominent contrasting effects that can reveal detailed physiological and biological information, and constitutes a new imaging category, known as manganese-enhanced MRI (MEMRI). In particular, MEMRI can help the visualization of the anatomic structure of the brain and its neuronal activity,[43] which cannot be obtained with any of the gadolinium(II)-based contrast agents. Unfortunately, however, MEMRI can only be applied in animal studies, because Mn^{2+} ions cause hepatic failure and have cardiac toxicity.

As shown above, the present T1 contrast agents are based on paramagnetic ions and are used in the form of ion complexes. They have short life spans in the body and work in a nonspecific manner. Most T1 contrast agents reside within the extracellular space, and usually interact with the blood so that they have some limitations as molecular probes for longer time tracking. As shown in recent studies of iron oxide nanoparticles, nanoparticulate agents are very promising for molecular and cellular imaging that aims to visualize the disease-specific biomarkers at the molecular and cellular levels, respectively. However, the negative contrasting effect and magnetic-susceptibility artifacts of iron oxide nanoparticles can be significant drawbacks when using iron oxide nanoparticles. This is because the resulting dark signal can mislead the clinical diagnosis in T2-weighted MRI, as the signal is often confused with the signals from bleeding, calcification, or metal deposits, and the susceptibility artifacts distort the background image.[9] Recently, intensive research has been devoted to developing new T1 contrast agents that overcome the above-mentioned drawbacks of Gd^{3+} ion- and Mn^{2+} ion-based T1 contrast agents and SPIO-based T2 contrast agents. Briefly, these new classes of contrast agents should satisfy the following characteristics: i) positive (T1) contrast ability, ii) easy intracellular uptake and accumulation for imaging cellular distribution and functions, iii) a nanoparticulate form for easy surface modification and efficient labeling with biological and bioactive materials, and iv) favorable pharmacokinetics and dynamics for easy delivery and efficient distribution to the biomarkers with minimal side effects.

The first class of particulate T1 contrast agents is based on nanostructured frames that have many anchoring sites for paramagnetic ions.[44] Those particles can carry a large number of paramagnetic payloads and produce strong T1 contrast. Various platforms, such as silicas, dendrimers, perfluorocarbons, emulsions, and nanotubes, have been used. Lanza and coworkers used perfluorocarbon nanoparticles incorporated paramagnetic Gd-DTPA complexes for the sensitive detection of fibrin and for the molecular detection of angiogenesis.[44a,b] Lin and coworkers developed silica nanoparticles,[44c] metal-organic frameworks,[44d] and mesoporous silica[44e] to contain a large number of Gd^{3+} ions and to develop multifunctional properties. Carbon nanotubes could act as the framework that holds Gd^{3+} ions, either on the surface[44f] or in the structural defect sites.[44g] In these materials, many metal ions are concentrated in a defined volume, and their biological behavior and relaxivities are different from those of the complex agents. Basically, this type of contrast agent is an extension of the paramagnetic complex agents so that the maximum number of ions is limited by the density of anchoring groups on the surface. Furthermore, the synthetic procedures are generally very complicated and expensive. The most significant limitation is their large overall size of >100 nm, which is much larger than that of inorganic nanoparticles, such as USPIO. To prevent easy excretion by the RES system and to compete with the small-sized T2 contrast agents, their overall size needs to be <100 nm, which is satisfied by inorganic nanoparticles.

Very recently, paramagnetic inorganic nanoparticles were developed as new T1 contrast agents. To be effective agents, the ratio between the transverse and longitudinal relaxivities (expressed as r_2/r_1), which is a defining parameter indicating whether the contrast agent can be employed as a positive or negative agent, has to be low.[20] That is, nanoparticles must have a large paramagnetic property (large r_1) with negligible magnetic anisotropy (small r_2). Nanoparticles of the many compounds of

Table 2. Properties of T1 contrast agents based on inorganic nanoparticles.

Name	Core Material	Surface	Diameter of Core [nm]	Hydrodynamic Diameter [nm]	Reference
Dextran-SPGO	Gd_2O_3	Dextran		26	45a
PEG-Gd_2O_3	Gd_2O_3	PEG	3		45b
GadoSiPEG	Gd_2O_3	Polysiloxane-PEG	2.2	3.3	45c
			3.8	5.2	
			4.6	8.9	
GdF_3:cit	GdF_3	Citric acid		129.3	46
GdF_3/LaF_3:AEP	GdF_3/LaF_3	2-Aminoethyl Phosphate		51.5	46
PGP/dextran-K01	$GdPO_4$	Dextran		23.2	47
MnO	MnO	PEG	7		48
			15		
			20		
			25		
FeCo/GC	FeCo	Graphitic Carbon-PEG	4	30	50
			7		

transition and lanthanide metals could be good candidates for T1 MRI contrast agents because the surface of the nanoparticles contains a large amount of metal ions with high magnetic moments. The most obvious nanoparticles for T1 agents are gadolinium-based ones, because many gadolinium complexes have been extensively used as clinical MRI contrast agents. Nanoparticles of gadolinium oxide (Gd_2O_3),[45] gadolinium fluoride (GdF_3),[46] and gadolinium phosphate ($GdPO_4$)[47] have been investigated as MRI contrast agents. They exhibited signal-enhancing contrast in T1-weighted images with low r_2/r_1 values. Tables 2 and 3 summarize the physical properties and relaxivities of some T1 contrast agents based on inorganic nanoparticles. The Gd_2O_3 nanoparticle-based agents are composed of small cores of <5 nm and stabilizing shells of dextran,[45a] PEG[45b], and silica[45c]. Bridot et al. reported the use of biocompatible gadolinium oxide nanoparticles with polysiloxane shells containing a fluorescent dye (GadoSiPEG2C) for in vivo dual imaging of magnetic resonance and fluorescence imaging (Fig. 10).[45c] Water-dispersible GdF_3 (or GdF_3/LaF_3) nanoparticles were prepared with either positively charged surfaces, by conjugation with 2-aminoethyl phosphate groups (GdF_3/LaF_3:AEP), or negatively charged surfaces, by coating with citrate groups (GdF_3:cit).[46] Dextran-coated $GdPO_4$ nanoparticles (PGP/dextran-K01) were synthesized by a hydrothermal process in the presence of dextran.[47] These Gd-based nanoparticles had significantly low r_2/r_1 values, and they showed strong positive-contrast effects. However, uniformly sized nanoparticles of gadolinium or related lanthanide compounds have not yet been demonstrated.

Very recently, MnO nanoparticles were developed as a new T1 MRI contrast agents for body organs such as the brain, liver, and kidney.[48] In particular, clear T1-weighted MR images of brain structures, depicting fine anatomic features, were obtained (Fig. 11). This clear anatomic imaging of the various brain structures can be utilized for many applications, such as basic neuroscience research and for the diagnosis of clinical neurological diseases

Table 3. Studies on r_1 relaxivities of T1 contrast agents based on inorganic nanoparticles.

Name	Core Material	Diameter of core [nm]	Relaxivity based on concentration of whole atoms		Relaxivity based on number of particles		Relaxivity based on surface		B_0 (T)	Reference
			r_1 [$mM^{-1}s^{-1}$]	r_2 [$mM^{-1}s^{-1}$]	r_1 [$mM^{-1}s^{-1}$]	r_2 [$mM^{-1}s^{-1}$]	r_1	r_2		
Gd-DTPA	Gd	ion	4.1	4.9	4.1	4.9			7	45c
Dextran-SPGO	Gd_2O_3		4.8	16.9					7	45a
PEG-Gd_2O_3	Gd_2O_3	3	9.4	13.4					1.5	45b
GadoSiPEG	Gd_2O_3	2.2	8.8	11.4	3700	4800			7	45c
		3.8	8.8	28.8	18600	60700				
		4.6	4.4	28.9	38800	65000				
PGP/dextran-K01	$GdPO_4$		13.9	15					0.47	47
GdF_3:cit	GdF_3		3.17		2.0×10^7		227.3[a]		14.2	46
GdF_3/LaF_3:AEP	GdF_3/LaF_3		2.71		8.8×10^5		77.2[a]		14.2	46
PGP/dextran-K01	$GdPO_4$		13.9	15					0.47	47
MnO	MnO	7	0.37	1.74	3000	14000	33[b]	154[b]	3	48
		15	0.18	0.57	15000	46000	34[b]	121[b]		
		20	0.13	0.52	25000	99000	33[b]	102[b]		
		25	0.12	0.44	46000	165000	39[b]	139[b]		
FeCo/GC	FeCo	4	31	185					1.5	50
		7	70	644						

[a] Relaxivities based on the Gd^{3+} on the shell (unit: $mM^{-1}s^{-1}$). [b] Relaxivities based on the surface area of nanoparticles (unit: $m\,s^{-1}$)

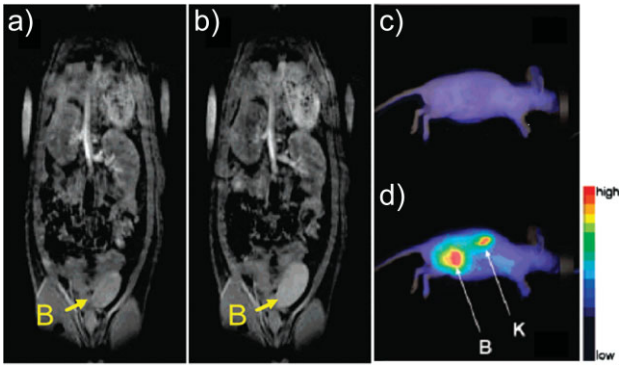

Figure 10. T1-weighted images of rat a) before and b) 1 h after injection of GadoSiPEG2C. Fluorescence reflectance imaging of a mouse c) before and d) 3 h after the injection of GadoSiPEG2C (K: kidneys, B: bladder). Reproduced with permission from [45c]. Copyright 2007 American Chemical Society.

(neurodegenerative diseases). Furthermore, functionalized MnO nanoparticles by conjugation with a tumor-specific antibody were used for the selective imaging of breast cancer cells in a metastatic brain tumor (Fig. 11c). Cancer cells were selectively enhanced in T1-weighted MRI because the functionalized MnO nanoparticles with tumor-specific antibody were delivered to and accumulated in the cancer cells with a clear marginal detectability without destroying the anatomic background. This clear marginal detectability while preserving the anatomic background images is a marked superiority of using a T1 over a T2 contrast agent.

Gilad et al. reported the labeling and tracking of rat glioma cells with either MnO nanoparticles or SPIO (Fig. 12).[49] Cells labeled with MnO nanoparticles and SPIO were each transplanted in contralateral brain hemispheres of a rat and tracked by in vivo MRI. SPIO-labeled cells showed a strong negative contrast in T2/T2*-weighted MRI. However, it is difficult to distinguish them from blood/hemosiderin-associated hypointense regions. MnO-labeled transplanted cells had a higher R1 than the brain tissue surrounding the transplanted cells. Therefore, MnO-labeled cells could be successfully detected and distinguished with positive contrast for in vivo T1-weighted MRI. The authors showed a MR "double labeling" technique using opposite contrasts simultaneously on two sites, where one is labeled with MnO and the other with SPIO nanoparticles. This labeling method can be applied to the tracking of cell populations that are injected in different locations or at different time points, by complementing and amplifying two kinds of contrasting effect.

Metal-alloy nanoparticles showed promising T1 contrasting effects, in particular for angiographic imaging agents. Dai and coworkers synthesized FeCo nanoparticles stabilized with single graphitic carbon shells (FeCo/GC) by chemical vapor deposition (Fig. 13).[50] After noncovalent functionalization with phospholipid–poly(ethylene glycol) (PL–PEG) molecules, the FeCo/GC nanoparticles became well dispersible and stable in aqueous media, and exhibited smaller r_2/r_1 values than the iron oxide nanoparticles and a large r_1 relaxivity. After their introduction into a rabbit, they showed successful in vivo intravascular T1 MRI, demonstrating long-circulating positive contrast enhancement ability of a nanoparticle-based contrast agent. Furthermore, the single-layered graphitic-carbon shell had strong near-infrared

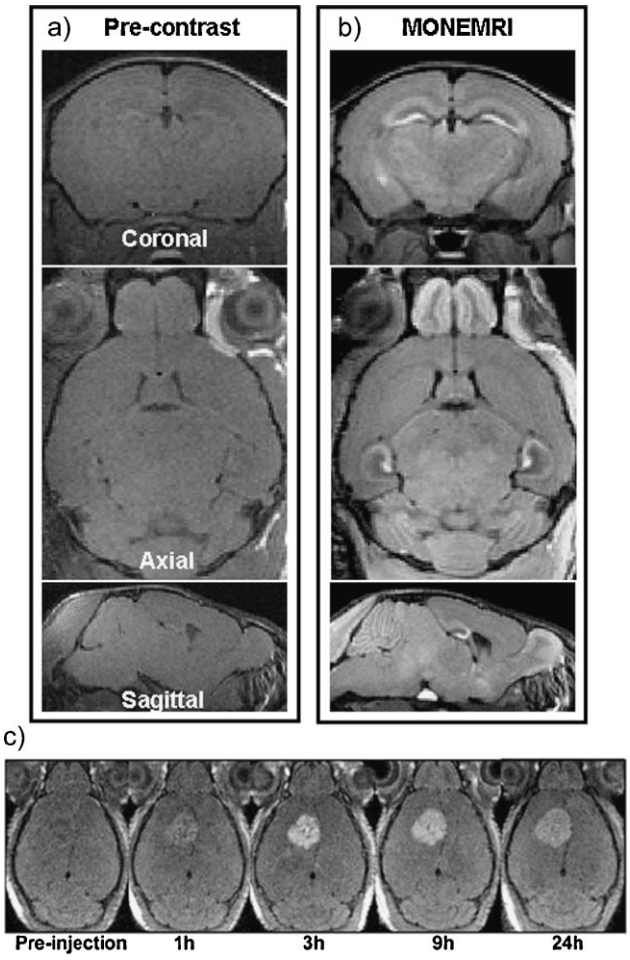

Figure 11. a,b)Typical coronal (top), axial (middle), and sagittal (bottom) views of a T1-weighted MONEMRI a) before and b) after the administration of the MnO nanoparticles. c) Breast-cancer cells were selectively enhanced in T1-weighted MRI by the Herceptin-functionalized MnO nanoparticles. Reproduced with permission from [48].

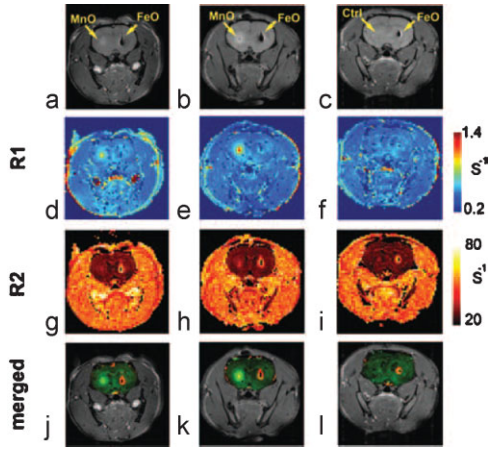

Figure 12. In vivo MRI of labeled rat glioma cells 24 h after transplantation in the striata of rat brain. a–c) Spin echo image. d–f) R1 maps. g–i) R2 maps. j–l) R1/R2 merged maps. MnO- and SPIO-labeled cells (a,b), and one with SPIO labeled cells and unlabeled cells (c; control). Reproduced with permission from [49].

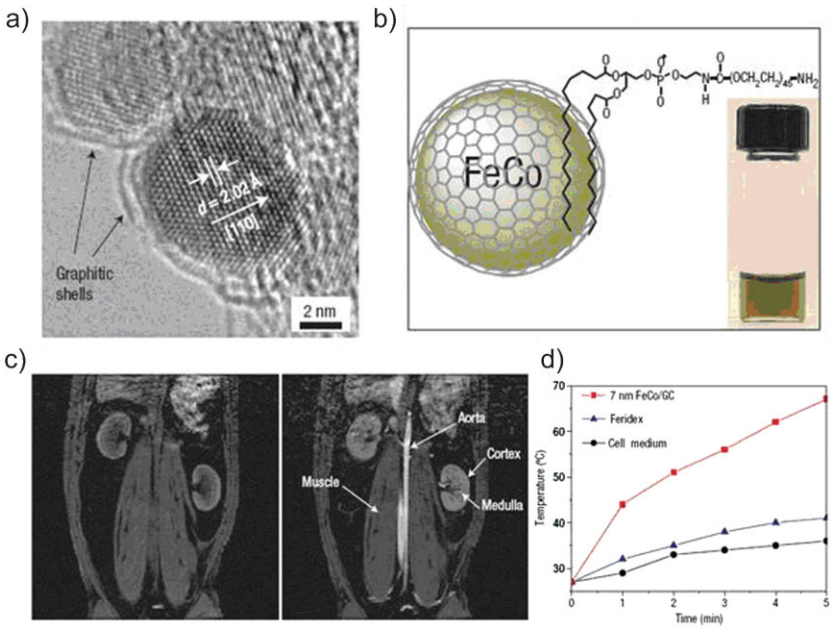

Figure 13. a) A high-resolution TEM image of FeCo nanoparticles with a graphitic shell. b) Schematic diagram of a FeCo/GC nanoparticles, structure of the phospholipid molecule used for functionalization, and a photograph of their suspension in PBS. c) T1-weighted MR images of a rabbit before (left) and 30 min after (right) initial injection of a solution of 4 nmFeCo/GC nanoparticles. d) Temperature-evolution curves for solutions of FeCo/GC and Feridex and control cell medium alone under continuous radiation of an 808 nm near-infrared laser. Reproduced with permission from [50]. Copyright 2006 Nature Publishing Group.

absorbance for the potential application to NIR photothermal therapy. Although the T1 contrasting mechanism of inorganic nanoparticle-based agents has not been fully elucidated yet, paramagnetic ions on the nanoparticle surface seem to be responsible for the relaxation enhancement of the protons near the nanoparticles.

4. New Non-Nanoparticulate Chemical-Exchange Saturation Transfer (CEST) Agents

In this report, we summarized the recent advances on the nanoparticulate MRI contrast agents. These nanoparticulate MRI contrast agents have progressed from previous ionic agents. For instance, nanoparticles of gadolinium oxide and manganese oxide were developed from the adaption of previous Gd^{3+}- and Mn^{2+}-based agents, respectively. Therefore, we expect that new classes of non-nanoparticulate agents can give motivation to the research on future nanoparticulate agents. In this section, we shortly introduce new classes of MRI contrast agents, CEST and paramagnetic CEST (PARACEST) agents.

4.1. CEST Agents

Recently, a new class of MRI contrast agents was proposed, so-called chemical exchange saturation transfer (CEST) agents, which can alter the signal of water protons through chemical exchange sites on the agent via saturation transfer.[51] CEST has attracted tremendous attention from many MRI scientists, because they can image metabolites in biological tissues as well as anatomy. It allowed monitoring of pH and detecting selectively endogenous amide protons, such as urea or ammonia, ex vivo and in vivo via the water resonance. Balaban and coworkers first showed the contrast in images generated by the metal-free exogenous agents, which consisted of diamagnetic molecules that contain exchangeable protons, such as –OH and –NH.[51a] The exchangeable protons in solutes or agents, which are in presaturation state, transfer the saturated magnetization to bulk water by strong irradiation of their resonance radio-frequency (RF) and through the exchange process, and this process leads to loss of bulk-water signal, which results in rendering an image dark. Many molecules possessing exchangeable protons, including sugars, amino acids, and metabolites, have been reported as exogenous agents. Among them, polypeptides and dendrimers, such as poly-L-lysine (PLL) and polyamiodoamine dendrimer, have been developed with sensitive enhancements due to the larger number of exchangeable protons.[51e]

Very recently, Gilad et al. reported a reporter gene that had an artificial sequence coding for lysine-rich protein (LRP) as an endogenous CEST agent in cells.[51f] As mentioned earlier, polypeptides that contain a large number of amides acted as concentrated exchangeable protons, and showed sensitive CEST. The authors demonstrated that LRP-expressing cells successfully showed contrast not only in cell extracts but in xenografts in mouse brains.

4.2. PARACEST Agents

Chemical-exchange saturation transfer depends on the difference of chemical shifts between an agent and water ($\Delta\omega$).[52a] There is, however, only a small difference (<5 ppm) between exchangeable protons of diamagnetic molecules and tissue water. Therefore, the research of CEST agents has been focused on the maximization of $\Delta\omega$ and the optimal k_{ex}. One approach is to utilize strong magnets on NMR or MRI because $\Delta\omega$ becomes large under high magnetic fields. High-field MRI is, however, not compatible with human clinical diagnosis yet. Therefore, recent researches have focused on the development of more efficient agents. The paramagnetic complexes, which have been used as traditional T1 contrast agents, induce a large chemical-shift difference and allow larger maximum values of exchange rates, which result in a more-effective contrasting effect.[52] For example, the water molecules coordinated on europium(III) ions are shifted to around 50 ppm, which is about 10-fold larger than the exchangeable protons of diamagnetic molecules. These lanthanide(III) paramagnetic chelates are called paramagnetic CEST (PARACEST) agents.

In particular, PARACEST agents produce distinctly different chemical shifts on different exchangeable protons, and enable to visualize them selectively with specific irradiation frequencies. Therefore, many researchers have developed PARACEST agents as ''smart'' agents. They image specific targets and respond to changes in the differences in molecular environments. These have been applied to monitor the biological activities such as pH, temperature, metabolites (arginine, lactate, glucose, or zinc), and enzyme activities. Representative PARACEST agents are the complexes of Eu^{3+} or Tb^{3+} formed with tetraamide derivatives of 1,4,7,10-tetraazacyclododecane-1,4,7,10-tetraacetic acid (DOTA).

Recent pursuit of higher sensitivity has rendered PARACEST agents as the form of supramolecular structures rather than simple complexes, as shown in previous achievements of T1 agents. Terreno and coworkers reported symmetrical chelates ($TmDOTP^{5-}$) coupled to cationic polymers (poly-L-argine) through charge–charge interactions.[52c] Nanosized carriers, such as liposomes[52d] and perfluorocarbon nanoparticles,[52e] were used to produce efficient PARACEST agents.

5. Conclusions and Outlook

Over last 20 years, various inorganic nanoparticles have been investigated as MRI contrast agents through the collaborative efforts of scientists working in materials science, biology, and medicine. Magnetic iron oxide nanoparticles have been extensively used as MRI contrast agents due to their ability to shorten T2* relaxation times in the liver, spleen, and bone marrow by selective uptake and accumulation in the RES cells. Depending on their particle sizes, iron oxide particle-based MRI contrasts are classified into MPIO, SPIO, and USPIO. Dextran-stabilized SPIOs have been clinically used for the diagnosis of liver diseases, including liver tumor, because SPIOs are selectively taken up by the Kupffer cells in the liver, spleen, and bone marrow. SPIOs have also been used for monitoring cell tracking and differentiation in cell therapy. On the other hand, USPIOs have been applied for lymph-node imaging. Iron oxide nanoparticles functionalized with bioactive materials, such as antibodies, peptides and oligonucleotides, have been used for targeted imaging via the site-specific accumulation of nanoparticles at the targets of interest. Conventionally, these SPIOs and USPIOs are prepared by the reduction and coprecipitation reaction of a mixture of ferrous and ferric salts in the presence of a hydrophilic polymer in aqueous media. More recently, uniform ferrite nanoparticles with high crystallinity have been synthesized from the thermal decomposition of metal precursors at high temperature in the presence of surfactants in organic media. Various surface-modification methods, including ligand exchange with water-dispersible ligands and encapsulation with biocompatible shells, have been developed to render these organic-dispersible nanoparticles water-dispersible and biocompatible. After proper surface treatment, these uniform ferrite nanoparticles have been successfully employed as new T2 MRI contrast agents with improved relaxation properties.

Recently, extensive research has been conducted to develop nanoparticle-based T1 contrast agents to overcome the drawbacks of iron oxide nanoparticle-based negative T2 contrast agents. Gadolinium complexes immobilized in various nanostructured materials, including nanoporous silicas, dendrimers, perfluorocarbon nanoparticles, and nanotubes, have been investigated as new T1 MRI contrast agents due to their ability to carry a large number of paramagnetic payloads and produce strong T1 contrast. More recently, nanoparticles of Gd_2O_3, GdF_3, and $GdPO_4$ have been investigated as T1 MRI contrast agents. Very recently, uniformly sized MnO nanoparticles were developed as a new T1 MRI contrast agent for body organs such as the brain, liver, and kidney. In particular, clear T1-weighted MR images of the brain structures, depicting fine anatomic structures, were obtained. The development of multifunctional platforms for either multimodal imaging or simultaneous imaging and therapy has been intensively pursued through the combinations of various nanomaterials.

As described above, most of the reported nanoparticle-based MRI contrast agents are still in the stage of in vitro testing or preliminary animal studies. Prior to their extensive use in clinic diagnosis, several key issues will have to be clearly addressed, including toxicological effects, long-term stability, and pharmacokinetics. Intensive interdisciplinary collaborative research is essential to achieve the ultimate goal of using nanoparticle-based MRI contrast agents for molecular and active imaging that can be applied to personalized diagnosis.

Acknowledgements

T. H. acknowledges financial support by the Korean Ministry of Education, Science and Technology through the National Creative Research Initiative Program of the Korea Science and Engineering Foundation (KOSEF).

Received: August 14, 2008
Revised: November 27, 2008
Published online: March 4, 2009

[1] *Encyclopedia of Imaging Science and Technology* (Ed: J. P. Hornak), Wiley-Interscience, New York **2002**.

[2] a) R. Weissleder, U. Mahmood, *Radiology* **2001**, *219*, 316. b) T. F. Massoud, S. S. Gambhir, *Genes Dev.* **2003**, *17*, 545. c) *Molecular and Cellular MR Imaging* (Eds: M. M. J, Modo, J. W. M. Bulte), CRC Press, Boca Raton, **2007**.

[3] P Caravan, J. J. Ellison, T. J. McMurry, R. B. Lauffer, *Chem. Rev.* **1999**, *99*, 2293.

[4] a) *Nanoparticles in Biomedical Imaging-Emerging Technologies and Applications* (Eds: J. W. M. Bulte, M. M. J. Modo), Springer, New York, **2008**. b) *Nanoscale Materials in Chemistry* (Ed: K. J. Klabunde), Wiley-Interscience, New York **2001**. c) A. P. Alivisatos, *Nat. Biotechnol.* **2004**, *22*, 47. d) J. Wang, *Small* **2005**, *1*, 1036. e) N. L. Rosi, C. A. Mirkin, *Chem. Rev.* **2005**, *105*, 1547. f) C. M. Niemeyer, *Angew. Chem. Int. Ed.* **2001**, *40*, 4128. g) *Nanomaterials for Medical Diagnosis and Therapy* (Ed: C. S. S. R. Kumar), Wiley-VCH, Weinheim **2007**. h) G. Schmid, *Nanoparticles: From Theory to Application*, Wiley-VCH, Weinheim, **2004**. i) C. M. Niemeyer, C. A. Mirkin, *Nanobiotechnology: Concepts, Applications and Perspectives*, Wiley-VCH, Weinheim **2004**. j) A. H. Lu, E. L. Salabas, F. Schüth, *Angew. Chem. Int. Ed.* **2007**, *46*, 1222.

[5] a) I. L. Medintz, H. T. Uyeda, E. R. Goldman, H. Mattoussi, *Nat. Mater.* **2005**, *4*, 435. b) X. Michalet, F. F. Pinaud, L. A. Bentolila, J. M. Tsay, S. Doose, J. J. Li, G. Sundaresan, A. M. Wu, S. S. Gambhir, S. Weiss, *Science* **2005**, *307*, 538. c) J. M. Klostranec, W. C. W. Chan, *Adv. Mater.* **2006**, *18*, 1953. d) B. Dubertret, P. Skourides, D. J. Norris, V. Noireaux, A. H.

Brivanlou, A. Libchaber, *Science* **2002**, *298*, 1759. e) M. Bruchez, Jr, M. Moronne, P. Gin, S. Weiss, A. P. Alivisatos, *Science* **1998**, *281*, 2013. f) W. C. W. Chan, S. Nie, *Science* **1998**, *281*, 2016. g) S. Kim, Y. T. Lim, E. G. Soltesz, A. M. De Grand, J. Lee, A. Nakayama, J. A. Parker, T. Mihaljevic, R. G. Laurence, D. M. Dor, L. H. Cohn, M. G. Bawendi, J. V. Frangioni, *Nat. Biotechnol.* **2004**, *22*, 93. h) K. E. Sapsford, L. Berti, I. L. Medintz, *Angew. Chem. Int. Ed.* **2006**, *45*, 4562. i) L. Medintz, A. R. Clapp, H. Mattoussi, E. R. Goldman, B. Fisher, J. M. Mauro, *Nat. Mater.* **2003**, *2*, 630. j) E. B. Voura, J. K. Jaiswal, H. Mattoussi, S. M. Simon, *Nat. Med.* **2004**, *2*, 993.

[6] a) M. C. Daniel, D. Astruc, *Chem. Rev.* **2004**, *104*, 293. b) C. A. Mirkin, R. L. Letsinger, R. C. Mucic, J. J. Storhoff, *Nature* **1996**, *382*, 607. c) X. Wu, H. Lu, J. Liu, K. N. Haley, J. A. Treadway, J. P. Larson, N. Ge, F. Peale, M. P. Bruchez, *Nat. Biotechnol.* **2003**, *21*, 41. d) T. A. Taton, C. A. Mirkin, R. L. Letsinger, *Science* **2000**, *289*, 1757. e) J. M. Nam, C. S. Thaxton, C. A. Mirkin, *Science* **2003**, *301*, 1884. Y. W. C. Cao, R. Jin, J. M. Mirkin, *Science* **2002**, *297*, 1536. f) S.-J. Park, T. A. Taton, C. A. Mirkin, *Science* **2002**, *295*, 1503. g) M. S. Han, A. K. R. Lytton-Jean, B.-K. Oh, J. Heo, C. A. Mirkin, *Angew. Chem. Int. Ed.* **2006**, *45*, 1807. h) P. Hazarika, B. Ceyhan, C. M. Niemeyer, *Small* **2005**, *1*, 844. i) C. M. Niemeyer, B. Ceyhan, P. Hazarika, *Angew. Chem. Int. Ed.* **2003**, *42*, 5766. j) C. M. Niemeyer, B. Ceyhan, *Angew. Chem. Int. Ed.* **2001**, *40*, 3685. k) N. L. Rosi, C. A. Mirkin, *Chem. Rev.* **2005**, *105*, 1547.

[7] M. A Brown, R. C. Semelka, *MRI: Basic Principles and Applications*, Wiley-Liss, New York **2003**.

[8] a) M. H. Mendonca Dias, P. C. Lauterbur, *Magn. Reson. Med.* **1986**, *3*, 328. b) R. C. Semelka, T. K. Helmberger, *Radiology* **2001**, *218*, 27.

[9] J. W. M. Bulte, D. L. Kraitchman, *NMR Biomed.* **2004**, *17*, 484.

[10] a) C. W. Jung, P. Jacobs, *Magn. Reson. Imaging* **1995**, *13*, 661. b) Y. X. Wang, S. M. Hussain, G. P. Krestin, *Eur. J. Radiol.* **2001**, *11*, 2319. c) P. Wunderbaldinger, L. Josephson, R. Weissleder, *Acad. Radiol.* **2002**, *9*, S304.

[11] M. G. Harisinghani, J. Barentsz, P. F. Hahn, W. M. Deserno, S. Tabatabaei, C. H. van de Kaa, J. de la Rosette, R. Weissleder, *N. Engl. J. Med.* **2003**, *348*, 2491.

[12] J. W. M. Bulte, T. Douglas, B. Witwer, S.-C. Zhang, E. Strable, B. K. Lewis, H. Zywicke, B. Miller, P. van Gelderen, B. M. Moskowitz, I. D. Duncan, J. A. Frank, *Nat. Biotechnol.* **2001**, *19*, 1141.

[13] A. S. Arbab, G. T. Yocum, H. Kalish, E. K. Jordan, S. A. Anderson, A. Y. Khakoo, E. J. Read, J. A. Frank, *Blood* **2004**, *104*, 1217.

[14] P. Walczak, D. A. Kedziorek, A. A. Gilad, S. Lin, J. W. M. Bulte, *Magn. Reson. Med.* **2005**, *54*, 769.

[15] a) L. Josephson, C.-H. Tung, A. Moore, R. Weissleder, *Bioconjugate Chem.* **1999**, *10*, 186. b) N. Hawrylak, P. Ghosh, J. Broadus, C. Schlueter, W. T. Greenough, P. C. Lauterbur, *Exp. Neurol.* **1993**, *121*, 181. c) M. Lewin, N. Carlesso, C.-H. Tung, X.-W. Tang, D. Cory, D. T. Scadden, R. Weissleder, *Nat. Biotechnol.* **2000**, *18*, 410. d) E. T. Ahrens, M. Feili-Hariri, H. Xu, G. Genove, P. A. Morel, *Magn. Reson. Med.* **2003**, *49*, 1006. e) I. J. de Vries, W. J. Lesterhuis, J. O. Barentsz, P. Verdijk, J. H. van Krieken, O. C. Boerman, W. J. Oyen, J. J. Bonenkamp, J. B. Boezeman, G. J. Adema, J. W. Bulte, T. W. Scheenen, C. J. Punt, A. Heerschap, C. G. Figdor, *Nat. Biotechnol.* **2005**, *23*, 1407.

[16] H. W. Kang, L. Josephson, A. Petrovsky, R. Weissleder, A. Bogdanov, Jr., *Bioconjugate Chem.* **2002**, *13*, 122.

[17] L. Josephson, M. F. Kircher, U. Mahmood, Y. Tang, R. Weissleder, *Bioconjugate Chem.* **2002**, *13*, 554.

[18] a) J. M. Perez, L. Josephson, T. O'Loughlin, D. Högemann, R. Weissleder, *Nat. Biotechnol.* **2002**, *20*, 816. b) R. Weissleder, K. Kelly, E. Y. Sun, T. Shtatland, L. Josephson, *Nat. Biotechnol.* **2005**, *23*, 1418.

[19] a) S. H. Koenig, K. E. Keller, *Magn. Reson. Med.* **1995**, *34*, 227. b) K. E. Kellar, D. K. Fujii, W. H. H. Gunther, K. Briley-Saebo, M. Spiller, S. H. Koenig, *Magn. Reson. Mater. Phys. Biol. Med.* **1999**, *8*, 207.

[20] a) J. Park, E. Lee, N.-M. Hwang, M. Kang, S. C. Kim, Y. Hwang, J.-G. Park, H.-J. Noh, J.-Y. Kim, J.-H. Park, T. Hyeon, *Angew. Chem. Int. Ed.* **2005**, *44*, 2872. b) Y.-W. Jun, Y.-M. Huh, J.-S. Choi, J.-H. Lee, H.-T. Song, S. Kim, S. Yoon, K.-S. Kim, J.-S. Shin, J.-S. Suh, J. Cheon, *J. Am. Chem. Soc.* **2005**, *127*, 5732.

[21] a) M. P. Morales, S. Veintemillas-Verdaguer, M. I. Montero, C. J. Serna, *Chem. Mater.* **1999**, *11*, 3058. b) Y.-W. Jun, J.-W. Seo, J. Cheon, *Acc. Chem. Res.* **2008**, *41*, 179. c) Y.-W. Jun, J.-H. Lee, J. Cheon, *Angew. Chem. Int. Ed.* **2008**, *47*, 5122.

[22] a) T. Hyeon, *Chem. Commun.* **2003**, 927. b) J. Park, J. Joo, S. G. Kwon, Y. Jang, T. Hyeon, *Angew. Chem. Int. Ed.* **2007**, *46*, 4630. c) J. Park, K. An, Y. Hwang, J.-G. Park, H.-J. Noh, J.-Y. Kim, J.-H. Park, N.-M. Hwang, T. Hyeon, *Nat. Mater.* **2004**, *3*, 891. d) U. Jeong, X. Teng, Y. Wang, H. Yang, Y. Xia, *Adv. Mater.* **2007**, *19*, 33.

[23] C. G. Hadjipanayis, M. J. Bonder, S. Balakrishnan, X. Wang, H. Mao, G. C. Hadjipanayis, *Small* **2008**, *4*, 1925.

[24] J.-H. Lee, Y.-M. Huh, Y-w. Jun, J-w. Seo, J-t. Jang, H.-T. Song, S. Kim, E.-J. Cho, H.-G. Yoon, J.-S. Suh, J. Cheon, *Nat. Med.* **2007**, *13*, 95.

[25] a) *Nanofabrication Towards Biomedical Applications: Techniques, Tools, Applications, and Impact* (Eds: S. S. R. Kumar, J. Hormes, C. Leuschner), Wiley-VCH, Weinheim **2005**. b) *Biofunctionalization of Nanomaterials* (Ed: C. Kumar), Wiley-VCH, Weinheim **2005**.

[26] a) C. Xu, K. Xu, H. Gu, R. Zheng, H. Liu, X. Zhang, Z. Guo, B. Xu, *J. Am. Chem. Soc.* **2004**, *126*, 9938. b) J. Xie, C. Xu, N. Kohler, Y. Hou, S. Sun, *Adv. Mater.* **2007**, *19*, 3163. c) M. Kim, Y. Chen, Y. Liu, X. Peng, *Adv. Mater.* **2005**, *17*, 1429. d) H. B. Na, I. S. Lee, H. Seo, Y. I. Park, J. H. Lee, S.-W. Kim, T. Hyeon, *Chem. Commun.* **2007**, 5167. e) S.-W. Kim, S. Kim, J. B. Tracy, A. Jasanoff, M. G. Bawendi, *J. Am. Chem. Soc.* **2005**, *127*, 4556.

[27] a) D. K. Yi, S. T. Selvan, S. S. Lee, G. C. Papaefthymiou, D. Kundaliya, J. Y. Ying, *J. Am. Chem. Soc.* **2005**, *127*, 4990. b) S. T. Selvan, P. K. Patra, C. Y. Ang, J. Y. Ying, *Angew. Chem. Int. Ed.* **2007**, *46*, 2448.

[28] T-. J Yoon, J. S. Kim, B. G. Kim, K. N. Yu, M.-H. Cho, J.-K. Lee, *Angew. Chem. Int. Ed.* **2005**, *44*, 1068.

[29] a) J. Kim, J. E. Lee, S. H. Lee, J. H. Yu, J. H. Lee, T. G. Park, T. Hyeon, *Adv. Mater.* **2008**, *20*, 478. b) Y. Ding, Y. Hu, X. Jiang, L. Zhang, C. Yang, *Angew. Chem. Int. Ed.* **2004**, *43*, 6369. c) Y. Ding, Y. Hu, L. Zhang, Y. Chen, X. Jiang, *Biomacromolecules* **2006**, *7*, 1766.

[30] J. Panyam, V. Labhasetwar, *Adv. Drug Delivery Rev.* **2003**, *55*, 329.

[31] a) C. G. Golander, J. N. Herron, K. Lim, P. Claesson, P. Stenius, J. D. Andrade, in: *Poly(ethylene glycol) Chemistry* (Eds. J. M. Harris), Plenum, New York **1992**, p. 221. b) R. Gref, Y. Minamitake, M. T. Peracchia, V. Trubetskoy, V. Torchilin, R. Langer, *Science* **1994**, *263*, 1600. c) D. Bazile, C. Prud'homme, M. Bassoullet, M. Marlard, G. Spenlehauer, M. Veillard, *J. Pharm. Sci.* **1995**, *84*, 493. d) M. Tobio, M. R. Gref, A. Sanchez, R. Langer, M. J. Alonso, *Pharm. Res.* **1998**, *15*, 270.

[32] L. E. W LaConte, N. Nitin, O. Zurkiya, D. Caruntu, C. J. O'Connor, X. Hu, G. Bao, *Magn. Reson. Imaging* **2007**, *27*, 1634.

[33] a) J. Qin, S. Laurent, Y. S. Jo, A. Roch, M. Mikhaylova, Z. M. Bhujwalla, R. N. Muller, M. Muhammed, *Adv. Mater.* **2007**, *19*, 1874. b) M. Gonzalesa, K. M. Krishnan, *J. Magn. Magn. Mater.* **2007**, *311*, 59.

[34] Y. Wang, J. F. Wong, X. Teng, X. Z. Lin, H. Yang, *Nano Lett.* **2003**, *3*, 1555.

[35] U. I. Tromsdorf, N. C. Bigall, M. G. Kaul, O. T. Bruns, M. S. Nikolic, B. Mollwitz, R. A. Sperling, R. Reimer, H. Hohenberg, W. J. Parak, S. Forster, U. Beisiegel, G. Adam, H. Weller, *Nano Lett.* **2007**, *7*, 2422.

[36] H. Maeda, J. Fang, T. Inutsuka, Y. Kitamoto, *Int. Immunopharmacol.* **2003**, *3*, 319.

[37] H. Lee, E. Lee, D. K. Kim, N. K. Jang, Y. Y. Jeong, S. Jon, *J. Am. Chem. Soc.* **2006**, *128*, 7383.

[38] F. Hu, L. Wei, Z. Zhou, Y. Ran, Z. Li, M. Gao, *Adv. Mater.* **2006**, *18*, 2553.

[39] C. Sun, O. Veiseh, J. Gunn, C. Fang, S. Hansen, D. Lee, R. Sze, R. G. Ellenbogen, J. Olson, M. Zhang, *Small* **2008**, *4*, 372.

[40] J. Kim, Y. Piao, T. Hyeon, *Chem. Soc. Rev.* **2009**, *38*, 372.

[41] a) C. Xu, J. Xie, D. Ho, C. Wang, N. Kohler, E. G. Walsh, J. R. Morgan, Y. E. Chin, S. Sun, *Angew. Chem. Int. Ed.* **2008**, *47*, 173. b) J.-S. Choi, Y.-W. Jun, S.-I. Yeon, H. C. Kim, J.-S. Shin, J. Cheon, *J. Am. Chem. Soc.* **2006**, *128*, 15982.

[42] Y. Piao, J. Kim, H. B. Na, D. Kim, J. S. Baek, M. K. Ko, J. H. Lee, M. Shokouhimehr, T. Hyeon, *Nat. Mater.* **2008**, *7*, 242.

[43] A. C. Silva, J. H. Lee, I. Aoki, A. P. Koretsky, *NMR Biomed.* **2004**, *17*, 532.

[44] a) S. Flacke, S. Fischer, M. J. Scott, R. J. Fuhrhop, J. S. Allen, M. McLean, P. Winter, G. A. Sicard, P. J. Gaffney, S. A. Wickline, G. M. Lanza, *Circulation* **2001**, *104*, 1280. b) P. M. Winter, A. M. Morawski, S. D. Caruthers, R. W. Fuhrhop, H. Zhang, T. A. Williams, J. S. Allen, E. K. Lacy, J. D. Robertson, G. M. Lanza, S. A. Wickline, *Circulation* **2003**, *108*, 2270. c) W. J. Rieter, J. S. Kim, K. M. L. Taylor, H. An, W. Lin, T. Tarrant, W. Lin, *Angew. Chem. Int. Ed.* **2007**, *46*, 3680. d) W. J. Rieter, K. M. L. Taylor, H. An, W. Lin, W. Lin, *J. Am. Chem. Soc.* **2006**, *128*, 9024. e) K. M. L. Taylor, J. S. Kim, W. J. Rieter, H. An, W. Lin, W. Lin, *J. Am. Chem. Soc.* **2008**, *130*, 2154. f) C. Richard, B.-T. Doan, J.-C. Beloeil, M. Bessodes, É. Tóth, D. Scherman, *Nano Lett.* **2008**, *8*, 232. g) B. Sitharaman, K. R. Kissell, K. B. Hartman, L. A. Tran, A. Baikalov, I. Rusakova, Y. Sun, H. A. Khant, S. J. Ludtke, W. Chiu, S. Laus, É. Tóth, L. Helm, A. E. Merbachd, L. J. Wilson, *Chem. Commun.* **2005**, *3915*.

[45] a) M. A. McDonald, K. L. Watkin, *Acad. Radiol.* **2006**, *13*, 421. b) M.-A. Fortin, R. M. Petoral, Jr, F. Söderlind, A. Klasson, M. Engström, T. Veres, P.-O. Käll, K. Uvdal, *Nanotechnology* **2007**, *18*, 395501. c) J.-L. Bridot, A.-C. Faure, S. Laurent, C. Rivière, C. Billotey, B. Hiba, M. Janier, V. Josserand, J.-L. Coll, L. V. Elst, R. Muller, S. Roux, P. Perriat, O. Tillement, *J. Am. Chem. Soc.* **2007**, *129*, 5076.

[46] F. Evanics, P. R. Diamente, F. C. J. M. van Veggel, G. J. Stanisz, R. S. Prosser, *Chem. Mater.* **2006**, *18*, 2499.

[47] H. Hifumi, S. Yamaoka, A. Tanimoto, D. Citterio, K. Suzuki, *J. Am. Chem. Soc.* **2006**, *128*, 15090.

[48] H. B. Na, J. H. Lee, K. An, Y. I. Park, M. Park, I. S. Lee, D.-H. Nam, S. T. Kim, S.-H. Kim, S.-W. Kim, K.-H. Lim, K.-S. Kim, S.-O. Kim, T. Hyeon, *Angew. Chem. Int. Ed.* **2007**, *46*, 5397.

[49] A. A. Gilad, P. Walczak, M. T. McMahon, H. B. Na, J. H. Lee, K. An, T. Hyeon, P. C. M. van Zijl, J. W. M. Bulte, *Magn. Reson. Med.* **2008**, *60*, 1.

[50] W. S. Seo, J. H. Lee, X. Sun, Y. Suzuki, D. Mann, Z. Liu, M. Terashima, P. C. Yang, M. V. Mcconnell, D. G. Nishimura, H. Dai, *Nat. Mater.* **2006**, *5*, 971.

[51] a) V. Guivel-Scharen, T. Sinnwell, S. D. Wolff, R. S. Balaban, *J. Magn. Reson.* **1998**, *133*, 36. b) K. M. Ward, A. H. Aletras, R. S. Balaban, *J. Magn. Reson.* **2000**, *143*, 79. c) J. Zhou, J.-F. Payen, D. A. Wilson, R. J. Traystman, P. C. van Zijl, *Nat. Med.* **2003**, *9*, 1085. d) N. Goffeney, J. W. M. Bulte, J. H. Duyn, L. H. Bryant, Jr, P. C. M. van Zijl, *J. Am. Chem. Soc.* **2001**, *123*, 8628. e) M. T. McMahon, A. A. Gilad, J. Zhou, P. Z. Sun, J. W. M. Bulte, P. C. M. van Zijl, *Magn. Reson. Med.* **2006**, *55*, 836. f) A. A. Gilad, M. T. McMahon, P. Walczak, P. T. Winnard Jr, V. Raman, H. W. M. van Laarhoven, C. M. Skoglund, J. W. M. Bulte, P. C. M. van zijl, *Nat. Biotechnol.* **2007**, *25*, 217.

[52] a) S. Zhang, M. Merritt, D. E. Woessner, R. E. Lenkinski, A. D. Sherry, *Acc. Chem. Res.* **2003**, *36*, 783. b) M. Woods, D. E. Woessner, A. D. Sherry, *Chem. Soc. Rev.* **2006**, *35*, 500. c) S. Aime, D. Delli Castelli, E. Terreno, *Angew. Chem. Int. Ed.* **2003**, *42*, 4527. d) S. Aim, D. Delli Castelli, E. Terreno, *Angew. Chem. Int. Ed.* **2005**, *44*, 5513. e) P. M. Winter, K. Cai, J. Chen, C. R. Adair, G. E. Kiefer, P. S. Athey, P. J. Gaffney, C. E. Buff, J. D. Robertson, S. D. Caruthers, S. A. Wickline, G. M. Lanza, *Magn. Reson. Med.* **2006**, *56*, 1384.